Article

Cell Reports

# Adenylosuccinate Is an Insulin Secretagogue Derived from Glucose-Induced Purine Metabolism

## Graphical Abstract

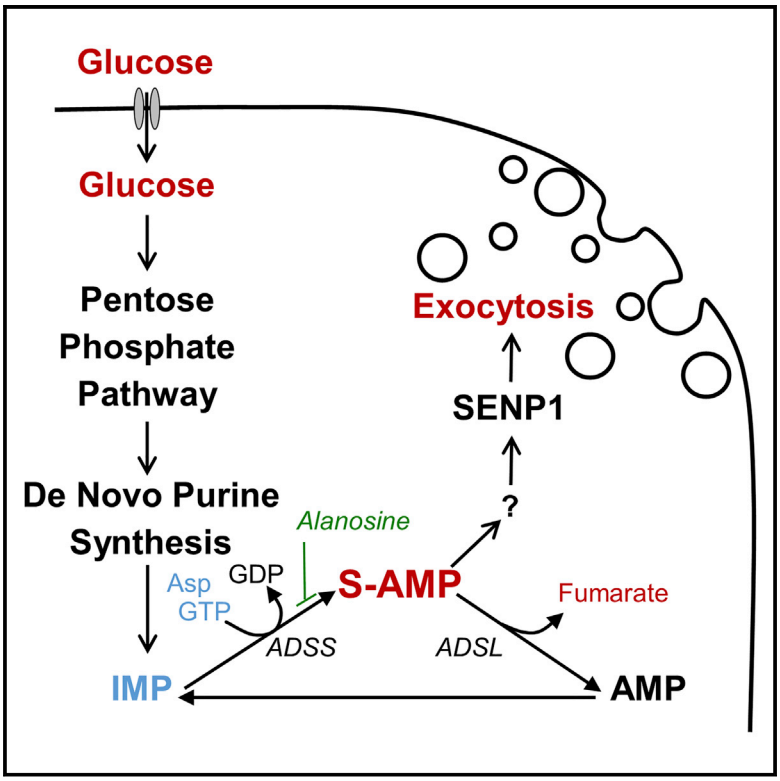


## Highlights

- Glucose stimulation increases the levels of adenylosuccinate (S-AMP) in β cells
- Interfering with S-AMP synthesis impairs glucose-stimulated insulin secretion
- Addition of S-AMP to patch-clamped human β cells stimulates insulin exocytosis
- S-AMP rescues secretory function in β cells from a human with type 2 diabetes

## Authors

Jessica R. Gooding, Mette V. Jensen, Xiaoqing Dai, ..., Mourad Ferdaoussi, Patrick E. MacDonald, Christopher B. Newgard

## Correspondence

pmacdonald@ualberta.ca (P.E.M.), chris.newgard@duke.edu (C.B.N.)

## In Brief

Loss of glucose-stimulated insulin from islet β cells heralds the onset of type 2 diabetes (T2D). Gooding et al. demonstrate a glucose-induced increase in a purine/nucleotide pathway intermediate, adenylosuccinate (S-AMP), and show that this metabolite is capable of stimulating insulin exocytosis in β cells obtained from normal and T2D humans.

Gooding et al., 2015, Cell Reports *13*, 157–167
October 6, 2015 ©2015 The Authors
http://dx.doi.org/10.1016/j.celrep.2015.08.072

Cell Reports
Article



# Adenylosuccinate Is an Insulin Secretagogue Derived from Glucose-Induced Purine Metabolism

Jessica R. Gooding,[1,3] Mette V. Jensen,[1,3] Xiaoqing Dai,[2] Brett R. Wenner,[1] Danhong Lu,[1] Ramamani Arumugam,[1] Mourad Ferdaoussi,[2] Patrick E. MacDonald,[2,4,*] and Christopher B. Newgard[1,4,*]
[1]Sarah W. Stedman Nutrition and Metabolism Center and Duke Molecular Physiology Institute, Departments of Pharmacology and Cancer Biology and Medicine, Duke University Medical Center, Durham, NC 27701, USA
[2]Alberta Diabetes Institute and Department of Pharmacology, University of Alberta, Edmonton, AB T6G 2E1, Canada
[3]Co-first author
[4]Co-senior author
*Correspondence: pmacdonald@ualberta.ca (P.E.M.), chris.newgard@duke.edu (C.B.N.)
http://dx.doi.org/10.1016/j.celrep.2015.08.072


## SUMMARY

**Pancreatic islet failure, involving loss of glucose-stimulated insulin secretion (GSIS) from islet β cells, heralds the onset of type 2 diabetes (T2D). To search for mediators of GSIS, we performed metabolomics profiling of the insulinoma cell line 832/13 and uncovered significant glucose-induced changes in purine pathway intermediates, including a decrease in inosine monophosphate (IMP) and an increase in adenylosuccinate (S-AMP), suggesting a regulatory role for the enzyme that links the two metabolites, adenylosuccinate synthase (ADSS). Inhibition of ADSS or a more proximal enzyme in the S-AMP biosynthesis pathway, adenylosuccinate lyase, lowers S-AMP levels and impairs GSIS. Addition of S-AMP to the interior of patch-clamped human β cells amplifies exocytosis, an effect dependent upon expression of sentrin/SUMO-specific protease 1 (SENP1). S-AMP also overcomes the defect in glucose-induced exocytosis in β cells from a human donor with T2D. S-AMP is, thus, an insulin secretagogue capable of reversing β cell dysfunction in T2D.**

## INTRODUCTION

Both type 1 and type 2 diabetes are diseases of insulin deficiency, albeit with different etiologies. Type 1 diabetes (T1D) occurs when pancreatic islet β cells are destroyed by the host immune system. Type 2 diabetes (T2D) involves loss of key β cell functions, such as glucose-stimulated insulin secretion (GSIS), coupled with gradual depletion of β cell mass by non-autoimmune mechanisms (Muoio and Newgard, 2008). A clearer understanding of β cell function is critical for ultimate success in the creation of surrogate cells for insulin replacement therapy in T1D and development of better drugs for enhancing β cell function in T2D. Here we have focused on metabolic coupling mechanisms in the β cell and how they are altered when islets fail in diabetes.

For over 30 years, one particular model of glucose stimulus/secretion coupling has gained wide acceptance. In this construct, glucose-driven increases in the ATP:ADP ratio inhibit ATP-sensitive $K^+$ channels ($K_{ATP}$ channels), resulting in plasma membrane depolarization, activation of voltage-gated $Ca^{2+}$ channels, and influx of extracellular $Ca^{2+}$, which serves to activate granule exocytosis (Bryan et al., 2005; Henquin et al., 2003; Newgard and Matschinsky, 2001). The $K_{ATP}$ channel-dependent mechanism appears to be particularly important in the first, acute phase of insulin release. In the second and sustained phase of insulin secretion, closure of $K_{ATP}$ channels is required as an initiating event, but does not fully explain the amplification of insulin secretion after initial glucose stimulation (Gembal et al., 1992; Sato et al., 1992; Straub and Sharp, 2002). In fact, amplifying signals contribute as much as 60% of total GSIS (Henquin et al., 2003), but mechanisms driving this component of the secretory response are still incompletely understood. Growing evidence implicates non-oxidative, anaplerotic metabolism of glucose as an important regulator of GSIS. In particular, the full GSIS response requires pyruvate carboxylase activity, efficient export of citrate and/or isocitrate from the mitochondria to the cytosol, and engagement of isocitrate with the cytosolic, NADP-dependent isocitrate dehydrogenase (IDH1 or ICDc) (Gooding et al., 2015; Ferdaoussi et al., 2015; Jensen et al., 2006, 2008; Joseph et al., 2006; Lu et al., 2002; Ronnebaum et al., 2006).

It has been recognized for some time that glucose stimulation of β cells causes broad-scale changes in an array of nucleotides and their biosynthetic precursors (Detimary et al., 1996). In our study, we applied a targeted liquid chromatography-tandem mass spectrometry (LC-MS/MS)-based method to probe this response in more detail. We found that exposure of the robustly glucose-responsive INS-1-derived insulinoma cell line 832/13 to stimulatory glucose concentrations results in a striking increase in adenylosuccinate (S-AMP) levels. Furthermore, molecular or pharmacological manipulation of S-AMP levels results in alterations in insulin secretion that are consistent with a regulatory role for this metabolite. Using patch-clamped human β cells and insulinoma cells, we were able to add S-AMP to the cell interior via the patch pipette. S-AMP enhances insulin granule exocytosis in 832/13 cells and non-diabetic human β cells,

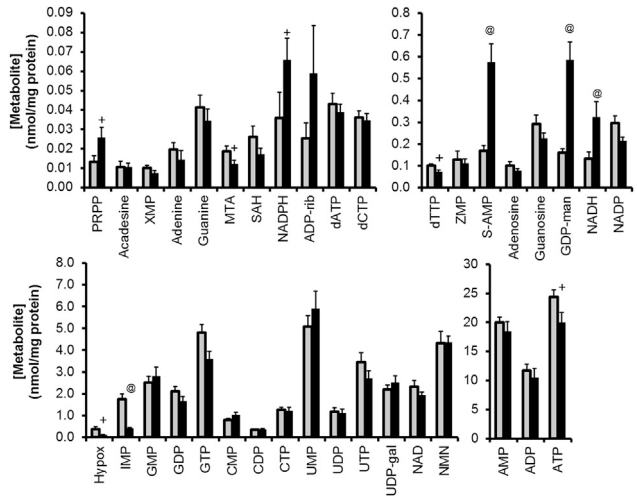


**Figure 1. Targeted Nucleotide Profiling of 37 Metabolites in 832/13 Cells**

The 832/13 cells were harvested after 2 hr exposure to either 2.5 mM (gray bars) or 12 mM (black bars) glucose and analyzed by LC-MS/MS for nucleotide content. Data are expressed as average ± SE of five independent experiments performed in triplicate. +$p < 0.05$ relative to 2.5 mM glucose; @$p < 0.01$ relative to 2.5 mM glucose as calculated by Wilcoxon rank-sum test. Full compound names and acquisition parameters for LC-MS/MS analyses are shown in Table S1.

and, when applied to β cells from a human donor with T2D, S-AMP completely reverses the defect in the glucose-dependent amplification of exocytosis. We also present evidence that S-AMP-mediated facilitation of granule exocytosis requires sentrin/SUMO-specific protease 1 (SENP1). These findings identify S-AMP as a metabolic intermediate that couples glucose metabolism to insulin secretion and that is able to reverse β cell dysfunction in T2D.

## RESULTS

### Glucose-Induced Changes in Purine Pathway Intermediates and Nucleotides

We applied a targeted LC-MS/MS assay method for measuring glucose-induced changes in 37 nucleotides and purine pathway intermediates in islet β cells. Our goal was to determine if any regulated metabolites could be ascribed a role in GSIS. Stimulation of the robustly glucose-responsive rat insulinoma cell line 832/13 with 12 mM glucose for 2 hr caused an increase in PRPP (1.9-fold, $p = 0.038$), but no detectable changes in other metabolites of early de novo purine synthesis (acadesine and 5-aminoimidazole-4-carboxamide ribonucleotide [ZMP]) relative to cells treated with basal glucose (2.5 mM glucose) (Figure 1). Glucose stimulation significantly changed the concentrations of intermediates later in the pathway, including inosine monophosphate (IMP) (77% decrease, $p = 1.3 \times 10^{-8}$), S-AMP (3.4-fold increase, $p = 4.0 \times 10^{-5}$), hypoxanthine (73% decrease, $p = 0.024$), and ATP (18% decrease, $p = 0.013$). Other purine (AMP, ADP, XMP, GMP, GDP, and GTP) and pyrimidine (CMP, CDP, CTP, UMP, UDP, and UTP) nucleotides did not change significantly in response to stimulatory glucose. Oxidized pyridines tended to decrease in concentration (NAD 16%; NADP 27%), whereas their reduced forms increased significantly (NADH 2.4-fold, $p = 0.009$; NADPH 1.8-fold, $p = 0.05$) in response to stimulatory glucose. Nucleotide conjugates GDP-mannose (3.7-fold increase, $p = 4.1 \times 10^{-6}$) and 5′-methylthioadenosine (MTA) (35% decrease, $p = 0.046$) also changed dynamically with glucose.

### MPA Inhibition of GSIS from 832/13 Cells Is Rescued by the Provision of Guanine

Inosine monophosphate dehydrogenase (IMPDH; *EC* 1.1.1.205) catalyzes the NAD-dependent conversion of IMP to XMP, and is considered to be the rate-limiting step in the de novo biosynthesis of guanine nucleotides. Two IMPDH isoforms are expressed in mammalian cells, encoded by distinct genes that share 84% amino acid identity and with similar catalytic activity (Carr et al., 1993; Hager et al., 1995; Natsumeda et al., 1990). The quantitative real-time PCR analysis of IMPDH mRNA levels in rat islets and 832/13 cells revealed that IMPDH2 is the more abundant isoform in both settings, being 6.7 ± 1.2-fold more abundant than IMPDH1 in rat islets (n = 4 independent islet samples, each measured in triplicate) and 9.7 ± 2.3-fold higher in 832/13 cells (n = 7 independent samples, each measured in duplicate). To test the role of the guanine arm of purine biosynthesis in the control of GSIS, we applied mycophenolic acid (MPA), a selective, reversible, and noncompetitive inhibitor of both isoforms of IMPDH (Kitchin et al., 1997), to 832/13 cells. MPA inhibited GSIS in a dose-dependent manner (Figure 2A). Co-culture with 100 μM guanine fully reversed the strong inhibitory effect of 2 μg/ml MPA on GSIS (Figure 2B), whereas 250 μM adenine caused only a minimal improvement.

### Effects of MPA on Nucleotide Levels

To further understand the inhibitory effect of MPA on GSIS and the discrete restorative effects of guanine versus adenine addition, we explored the effects of these agents on nucleotide pools in 832/13 cells exposed to 12 mM glucose (Figures 2C and S1). As expected, treatment with 2 μg/ml MPA caused increases in upstream purine pathway intermediates, such as PPRP, acadesine, ZMP, and IMP (all $p \leq 0.05$). Also as expected, metabolites in the guanine nucleotide pathway, including guanosine, GMP, GDP, and GTP, decreased in response to the inhibition of IMPDH with MPA (all $p < 0.05$). Surprisingly, MPA-treated cells also had lower levels of adenine metabolites, including S-AMP, AMP, ADP, and ATP (all $p < 0.05$), demonstrating that a block in the guanine metabolic pathway impacts production of intermediates of adenine metabolism.

Consistent with their divergent effects on rescue of GSIS in MPA-treated cells, guanine and adenine addition had discrete effects on purine and nucleotide metabolites when added in the presence of MPA. Under these conditions, both guanine and adenine addition lowered the levels of the precursor metabolites PRPP, acadesine, and ZMP back to levels observed in control cells or lower. In the presence of MPA plus adenine, levels of guanosine, GMP, GDP, GTP, S-AMP, AMP, ADP, and ATP were all lower than in control cells (no MPA, no nucleobase addition), with $p < 0.01$ (Figure 2C). In contrast, all of the foregoing analytes were equal to or greater than control in the presence

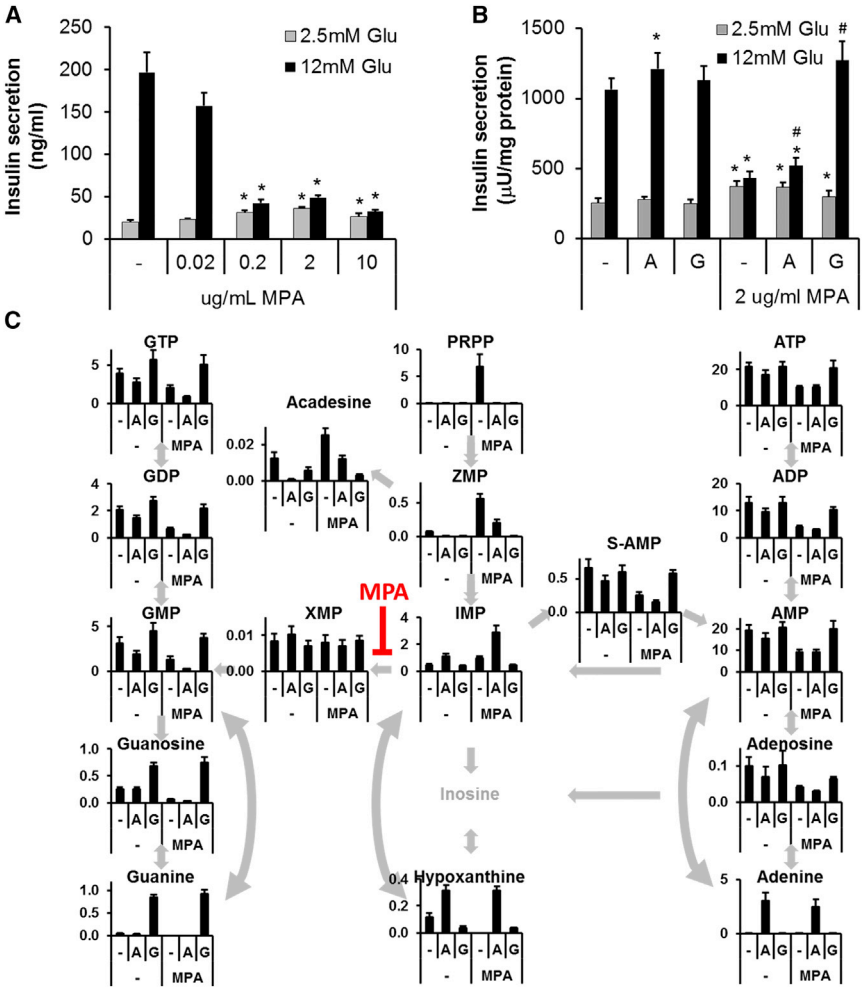


**Figure 2. Guanine, but Not Adenine, Rescues the Inhibitory Effects of MPA on GSIS and Purine Metabolites**

(A and B) Insulin secretion from 832/13 cells measured (A) in the presence or absence of mycophenolic acid (MPA) addition or neither (ON), during preincubation and GSIS; and (B) with or without adenine (250 μM) or guanine (100 μM) addition in combination with MPA. Data are expressed as average ± SE of three independent experiments performed in triplicate. *$p < 0.05$ relative to no MPA; #$p < 0.05$ relative to +MPA.

(C) The 832/13 cells were treated with MPA (2 μg/ml) in the presence of adenine (A) or guanine (G), or neither (–), during preincubation and glucose stimulation (12 mM). Purine concentrations were quantified by LC-MS/MS. Data are expressed as average ± SE in nmol metabolite/mg protein of three independent experiments performed in triplicate. See Figure S1 for quantification of additional metabolites.

of MPA plus guanine. In other words, guanine, but not adenine, was able to reverse the effects of MPA to lower these metabolites, in concert with guanine's unique ability to rescue GSIS.

## Pharmacologic Inhibition and siRNA-Mediated Suppression of ADSS Impairs GSIS

One potential explanation for the surprising effect of guanine to rescue adenine nucleotide pools and GSIS is that GTP is a cofactor for adenylosuccinate synthase (ADSS; EC 6.3.4.4), which catalyzes conversion of IMP and aspartic acid to S-AMP. In mammals, two isozymes are present. ADSS1 is highly abundant in cardiac and skeletal muscle tissues and is thought to play a role in energy metabolism via the purine nucleotide cycle. ADSS2 is present at low levels in most tissues and functions in de novo AMP biosynthesis (Stayton et al., 1983). Interestingly, ADSS2 is more abundant than ADSS1 in rat islets and 832/13 cells, with 26 ± 5-fold more ADSS2 than ADSS1 mRNA in rat islets, and 15 ± 1-fold more in 832/13 cells. To test the role of ADSS in GSIS, we treated 832/13 cells with small interfering RNA (siRNA) duplexes specific for ADSS1 and ADSS2, resulting in 71% ± 3% and 84% ± 3% decreases in mRNA expression, respectively (Figure 3A). These manipulations had no effect on basal insulin output (Figure 3B), but knockdown of ADSS2 caused 38% and 29% decreases in insulin secretion at 12 mM glucose compared to mock-transfected (no duplex [ND]) cells or cells treated with a control siRNA duplex (siCont), respectively ($p < 0.01$ for both controls). In cells treated with siADSS1, insulin secretion at 12 mM glucose was reduced relative to ND ($p < 0.01$) but did not reach significance relative to siCont ($p = 0.094$). Simultaneous knockdown of ADSS1 and ADSS2 (by 63% ± 8% and 78% ± 4% compared to ND, respectively) suppressed GSIS to the same extent as knockdown of ADSS2 alone. These findings were confirmed with a second set of siRNA duplexes targeting ADSS1 and ADSS2 (data not shown).

When added to cells, alanosine is converted by SAICAR synthase to 5-amino-4-imidazole carboxylic acid, a powerful and selective inhibitor of ADSS (Ki ~0.3 μM) (Jayaram et al., 1979). We therefore determined if the inhibitory effects of siADSS duplexes on GSIS were recapitulated by alanosine exposure. Treatment of 832/13 cells with 20 μg/ml alanosine significantly reduced insulin secretion at 12 mM glucose ($p < 0.001$) without affecting basal insulin secretion ($p = 0.7$) (Figure 3D). Alanosine also had a dose-dependent effect to inhibit GSIS in primary rat islets, with a 15% decrease at 20 μg/ml and a 40% decrease at 100 μg/ml at stimulatory glucose (16.7 mM) (Figure 3C). Provision of adenine completely reversed the inhibitory effect of 20 μg/ml alanosine on GSIS in 832/13 cells ($p < 0.01$).

## Effects of Alanosine on Nucleotide Levels

To explore the mechanism of alanosine inhibition on GSIS, we performed nucleotide profiling in 832/13 cells treated overnight and during the insulin secretion assay with 20 μg/ml alanosine

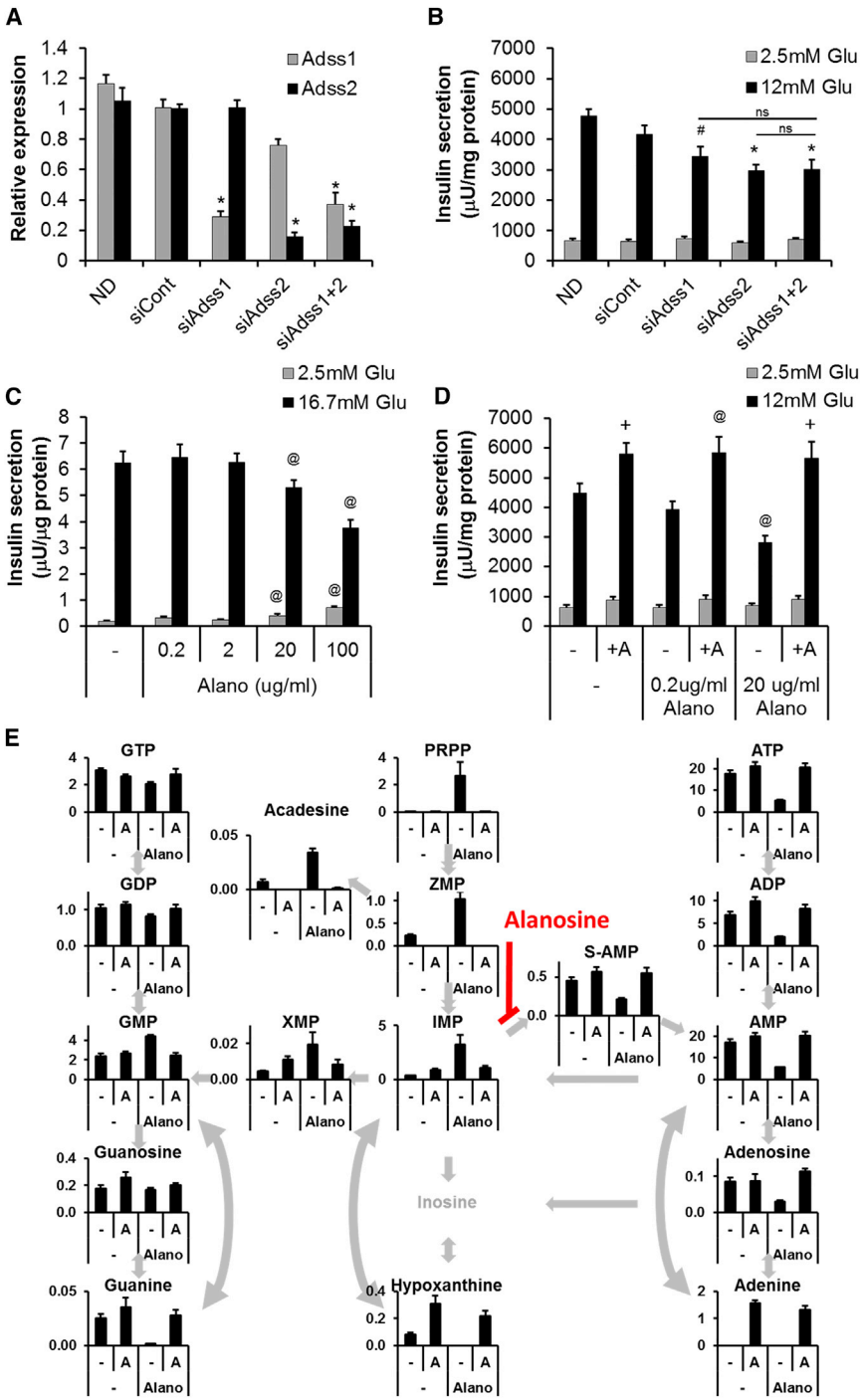


**Figure 3. Pharmacologic or Molecular Inhibition of ADSS Expression Impairs GSIS**

(A and B) The 832/13 cells were mock-transfected (ND), or transfected with either a control siRNA (siCont) or siRNA duplexes targeting ADSS1 or 2, and kept in culture for 72 hr prior to (A) quantitative real-time PCR analyses or (B) insulin secretion analyses. *p < 0.01 relative to ND and siCont; #p < 0.01 relative to ND.

(C and D) Insulin secretion from primary rat islets (C) or 832/13 cells (D) incubated with various doses of alanosine (alano) for 20 hr in the presence (+A) or absence (–) of adenine. +p < 0.05 relative to no alanosine control; @p < 0.01 relative to no alanosine control. Data in (A)–(D) represent the average ± SE of three to four independent experiments performed in triplicate.

(E) The 832/13 cells were treated with alanosine (20 μg/ml) in the presence (A) or absence (–) of adenine (100 μM) or during preincubation and glucose stimulation (12 mM), as indicated. Purine concentrations were quantified by LC-MS/MS. Data are expressed as average ± SE in nmol metabolite/mg protein for two independent experiments performed in triplicate. See Figure S2 for quantification of additional metabolites.

(Figures 3E and S2). As anticipated, inhibition of ADSS with alanosine caused increases in upstream metabolites such as PRPP, ZMP, acadesine, and IMP (all $p < 0.05$). ADSS inhibition also decreased the concentration of its enzyme product, S-AMP, by 52% ($p = 0.0022$), as well as the pools of downstream products adenosine, AMP, ADP, and ATP (all $p < 0.01$). Some products of the guanine pathway tended to increase in alanosine-treated cells (XMP 4.3-fold, $p = 0.26$; GMP 1.9-fold, $p = 0.0022$), indicating that ADSS inhibition may cause some diversion of IMP through the IMPDH reaction.

The addition of 100 μM adenine to alanosine-treated cells lowered the concentrations of upstream metabolites (PRPP, ZMP, and acadesine) back to or below the levels of controls, and raised downstream metabolite concentrations (S-AMP, adenosine, AMP, ADP, and ATP) back to control levels.

## S-AMP Is Rapidly Induced by Glucose and Augments Depolarization-Induced Exocytosis in 832/13 Cells

In evaluating our nucleotide profiling data, we were particularly intrigued with the 3.4-fold increase in S-AMP in response to stimulatory glucose, because this increase was in the opposite direction of metabolites directly upstream (IMP 77% decrease, aspartate 59% decrease) in its metabolic pathway, and in the same direction as its degradation product fumarate (Ferdaoussi et al., 2015; Jensen et al., 2006). These findings implicate S-AMP as a candidate stimulus/secretion coupling factor. Also supporting this idea, GSIS was impaired in response to molecular or pharmacologic suppression of ADSS, the enzyme that generates S-AMP (Figure 3). Moreover, S-AMP levels were rescued by the provision of guanine in MPA-treated cells and adenine in

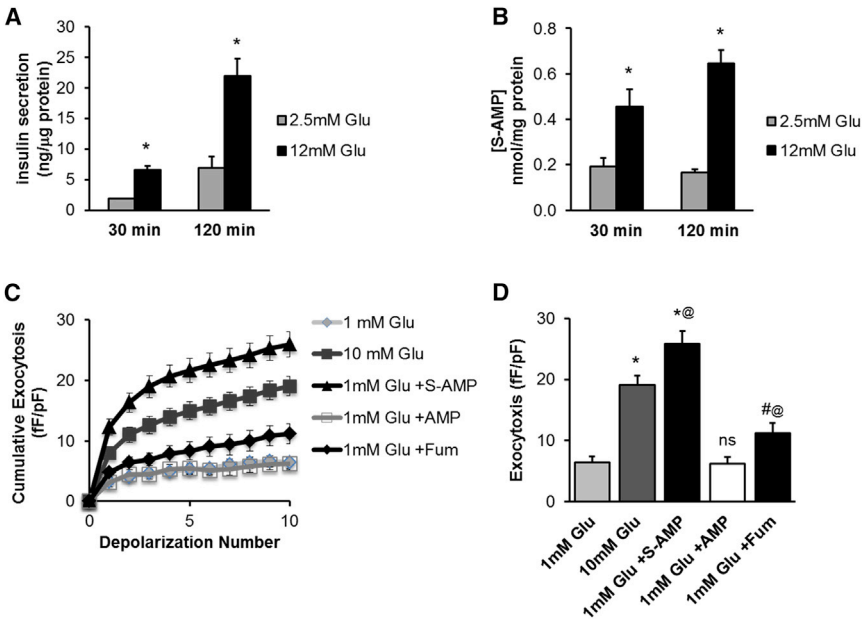


**Figure 4. Time Course of Glucose-Stimulated S-AMP Changes and Effect of S-AMP to Augment the Exocytotic Response of 832/13 Cells to Membrane Depolarization**

(A and B) GSIS (A) and changes in S-AMP levels (B) in 832/13 cells incubated at basal (2.5 mM) or stimulatory (12 mM) glucose for 30 or 120 min (n = 2 independent experiments, each assayed in triplicate and expressed as average ± SE; *p < 0.001 compared to basal glucose).

(C and D) Cumulative exocytosis over ten depolarizations (C) and the total exocytotic response (D) in 832/13 cells following acute glucose (10 mM) exposure, or upon infusion of S-AMP (10 μM), AMP (10 μM), or fumarate (10 μM) (n = 22, 24, 26, 19, and 20 cells, respectively). Data are expressed as average ± SE. *p < 0.01 and #p < 0.05 compared to basal glucose; @p < 0.05 compared to 10 mM glucose; ns, not significant.

alanosine-treated cells, in concert with the rescue of GSIS in both cases (Figures 2 and 3).

As a first step in evaluating S-AMP as a potential coupling factor for insulin secretion, we sought better understanding of the time course of its response to glucose, since all of the nucleotide profiling shown in Figures 1, 2, and 3 was performed after 2 hr of exposure to basal or stimulatory glucose. If S-AMP is relevant as an insulin secretagogue, its levels should increase at time points at which insulin secretion is initiated, earlier than 2 hr. We therefore performed measurements of GSIS and S-AMP levels at 30 min and 120 min in 832/13 cells incubated at basal (2.5 mM) and stimulatory (12 mM) glucose. We observed robust stimulation of GSIS (Figure 4A) in concert with strong and significant increases in S-AMP at both time points (Figure 4B). These data show that S-AMP levels are responsive to glucose over a time frame that is consistent with a role for this metabolite in the regulation of GSIS.

S-AMP is not expected to be membrane permeant, so in order to test its potential role as an insulin secretagogue, we performed patch-clamp studies on 832/13 cells using membrane capacitance as a measure of insulin granule exocytosis (Kanno et al., 2004). With this system, compounds such as S-AMP can be readily introduced to the interior of the cell via the patch pipette. In patch-clamped 832/13 cells, we observed a 2.9-fold amplification of exocytosis in cells pre-treated with 10 mM compared with 1 mM glucose (Figures 4C and 4D; n = 22–24 cells, p < 0.001). Remarkably, when tested in the presence of 1 mM glucose, 10 μM S-AMP was an even more potent facilitator of exocytosis than 10 mM glucose, resulting in a 4.1-fold increase in the exocytotic response relative to 1 mM glucose alone (Figures 4C and 4D; n = 26 cells, p < 0.001). S-AMP was further metabolized to yield AMP and fumarate by adenylosuccinate lyase (ADSL). Consistent with a specific effect of S-AMP on exocytosis, 10 μM AMP had no significant effect on exocytosis (n = 19 cells, p = 0.9), whereas 10 μM fumarate increased exocytosis 1.8-fold over basal levels (n = 19 cells, p < 0.05), a significant but clearly lesser effect compared to glucose or S-AMP (p < 0.01; Figures 4C and 4D).

## Suppression of ADSL Expression Lowers S-AMP and Impairs GSIS

ADSL plays two important roles in nucleotide metabolism, serving first to catalyze a proximal step in the purine biosynthetic pathway, the conversion of SAICAR to AICAR (ZMP), and then also acting to degrade S-AMP to AMP and fumarate more distally. Since knockdown of ADSL could slow biosynthesis of S-AMP and/or inhibit its degradation, with no certain net outcome, we decided to test the effect of siRNA-mediated suppression of the enzyme directly. Accordingly, we used an siRNA duplex to suppress ADSL mRNA levels by approximately 50% in 832/13 cells, resulting in clear impairment of GSIS (Figure 5A). Consistent with a dominant role of ADSL in proximal steps of the purine pathway, ADSL knockdown also caused a clear decrease in S-AMP levels at stimulatory glucose levels (Figure 5B). Unlike inhibition of IMPDH or ADSS, ADSL knockdown did not result in decreases in other adenine nucleotides (AMP, ADP, and ATP; Figure 5B) or GTP (data not shown), and in fact caused small increases in AMP, ADP, and ATP levels (Figure 5B). These data are consistent with a regulatory role of S-AMP in GSIS that is independent of other nucleotides.

## Effects of S-AMP on Exocytosis in β Cells from Non-diabetic Human Donors

Next, we investigated if the effect of S-AMP on exocytosis in 832/13 cells extrapolates to primary human β cells. In dispersed and reaggregated islet cells from normal (non-diabetic) donors, insulin secretion was increased by 3.3-fold in response to 16.7 mM glucose relative to 2.5 mM glucose (Figure 6A). Patch clamping of β cells from the same donors following an acute (~10–15 min) increase of glucose from 1 to 10 mM revealed a 2.2-fold increase in depolarization-induced exocytosis (n = 15–17

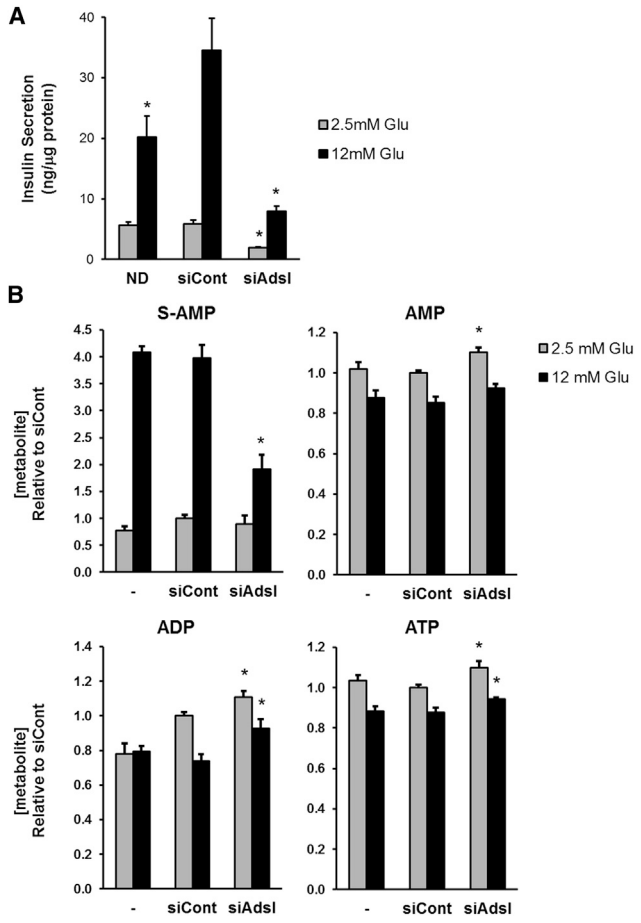


**Figure 5. Effect of ADSL Knockdown on GSIS, S-AMP, and Adenine Nucleotide Levels**

The 832/13 cells were treated with an siRNA duplex specific for ADSL (siAdsl), resulting in an ~50% decrease in ADSL mRNA levels compared to cells treated with a nontargeting siRNA (siCont) or untreated cells (ND).

(A) The effect of ADSL knockdown on GSIS is shown.

(B) Changes in S-AMP, AMP, ADP, and ATP in ND, siCont, and SiAdsl cells are shown. For all, n = 2 independent experiments, each assayed in triplicate and expressed as average ± SE. *p < 0.05 compared to siCont for the same glucose level.

cells from three donors; Figure 6B). Intracellular dialysis with 10 μM S-AMP amplified the exocytotic response to membrane depolarization-induced $Ca^{2+}$ entry by 3-fold compared to 1 mM glucose alone (Figure 6B; n = 20 cells from three donors, p < 0.01). Taken together, our results identify S-AMP as a glucose-regulated intermediate of nucleotide metabolism that enhances insulin granule exocytosis stimulated by membrane depolarization in human β cells and rodent insulinoma cells.

## The Amplifying Effect of S-AMP on Exocytosis Is Dependent on SENP1

Cellular proteins can be modified by SUMOylation, the covalent attachment of small ubiquitin-like modifier (SUMO) peptides. These processes are reversed by the deSUMOylation enzymes known as sentrin/SUMO-specific proteases (SENPs) (Yeh, 2009). In β cells, insulin granule exocytosis is impaired by SUMOylation, and nutrient stimulation activates SENP1 to remove these modifications and activate secretion (Dai et al., 2011; Vergari et al., 2012; Ferdaoussi et al., 2015). To determine whether the amplifying effect of S-AMP on exocytosis is dependent on SENP1 activity, we used siRNA to suppress SENP1 expression in human β cells from non-diabetic donors, leading to a 62% decrease in SENP1 mRNA levels relative to siCont-treated cells (n = 6 and 6 cells, respectively, from three donors, p < 0.01). This treatment resulted in a 58% decline in the exocytotic response following 10 mM glucose treatment compared to siCont-treated cells (Figure 6C; n = 17 and 16 cells, respectively, from three donors, p < 0.01). Similarly, knockdown of SENP1 reduced the S-AMP-dependent facilitation of exocytosis by 50% (Figure 6C; n = 25 and 20 cells from three donors, p < 0.01), indicating that the full amplifying effect of S-AMP requires SENP1 activity.

## S-AMP Rescues Impaired Exocytosis in Human T2D β Cells

Given the potent effects of S-AMP to enhance exocytosis in 832/13 cells and β cells from non-diabetic human donors, we investigated the effects of S-AMP in β cells from a human T2D donor. As expected, the GSIS response measured in islet cell aggregates from the T2D donor was impaired relative to secretion from human islet cell aggregates from non-diabetic donors (1.6-fold versus 3.3-fold, compare Figures 6A and 6D). Similarly, 10 mM glucose failed to potentiate depolarization-induced exocytosis compared to 1 mM glucose in β cells from the T2D donor (n = 8–9 cells, p = 0.6; Figure 6E). However, dialysis of 10 μM S-AMP induced an approximate 2.5-fold amplification of depolarization-induced exocytosis in the T2D β cells (Figure 6E; n = 8 cells, p < 0.01), similar to the effect of S-AMP or stimulatory glucose in normal human β cells (Figure 6B). Thus, our data demonstrate that, in addition to amplifying the exocytotic response in non-diabetic human β cells, S-AMP rescues dysfunctional exocytosis in human T2D β cells.

## DISCUSSION

Glucose metabolism contributes to purine and nucleotide biosynthesis via entry of glucose into the pentose monophosphate shunt to form ribose-5-P, on which the ring structures of nucleotides are synthesized from glycine, glutamine, aspartate, and 10-formyltetrahydrofolate. Several recent studies have used metabolomics to document changes in an array of purine and nucleotide pathway intermediates in response to glucose challenge in the INS-1-derived 832/13 β cell line created in our laboratory (Huang and Joseph, 2014; Lorenz et al., 2013; Spégel et al., 2011). These findings provide correlative data suggesting that some of the metabolites could function as stimulus/secretion coupling factors, but direct experiments to test individual candidate mediators have not appeared. To delve deeper into this possibility, we employed a targeted, quantitative LC-MS/MS method for survey of purine and nucleotide pathway intermediates. Using this method, we found a decrease in IMP, and an increase in S-AMP in glucose-stimulated 832/13 cells, suggesting that the enzyme linking the two metabolites, ADSS, could play a regulatory role in β cell glucose sensing. Although the

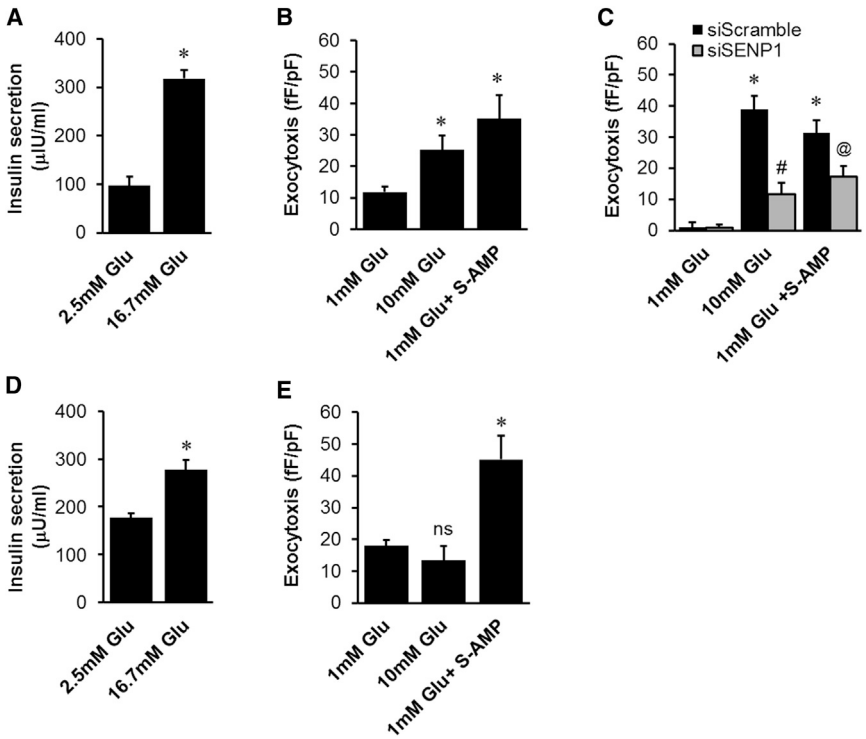


**Figure 6. S-AMP Increases the Exocytotic Response of Human β Cells to Membrane Depolarization in an SENP1-Dependent Manner and Rescues Impaired Exocytosis in Human T2D β cells**

(A) GSIS from islet cell aggregates from non-diabetic human donors is shown.

(B) The total exocytotic response of non-diabetic human β cells following acute glucose (10 mM) stimulation or upon infusion of 10 μM S-AMP is shown (n = 15, 17, and 20 cells from three donors).

(C) The total exocytotic response of non-diabetic human β cells transfected with control duplex (siScrambled; n = 14, 17, and 25 cells from three donors) or a duplex targeting SENP1 (siSenp1, n = 13, 16, and 20 cells from three donors), following acute glucose (10 mM) stimulation or after administration of 10 μM S-AMP, is shown.

(D) GSIS from islet cell aggregates from a human donor with T2D is shown.

(E) The total exocytotic response of human β cells from a T2D donor following acute glucose (10 mM) stimulation, or upon infusion of 10 μM S-AMP is shown (n = 9, 8, and 8 cells from one donor). Data are expressed as average ± SE. *$p < 0.01$ compared with the basal glucose condition; #$p < 0.01$ compared to siScrambled/10 mM glucose; @$p < 0.05$ compared to siScrambled/S-AMP.

glucose-induced decrease in IMP has been reported previously (El-Azzouny et al., 2014), this is the first finding of changes in levels of S-AMP in β cells in response to glucose stimulation. Consistent with the concept that ADSS and its product S-AMP have a stimulus/secretion coupling role, pharmacologic or molecular suppression of ADSS caused impairment of GSIS with attendant decreases in S-AMP, effects that could be overcome by the addition of adenine. Moreover, siRNA-mediated suppression of ADSL, a more proximal enzyme in the S-AMP biosynthetic pathway, impaired GSIS and lowered S-AMP levels, independent of decreases in other adenine nucleotides or GTP. Strikingly, infusion of S-AMP into patch-clamped 832/13 cells or β cells from non-diabetic human subjects stimulated exocytosis at least as well as glucose, and S-AMP also rescued exocytosis in glucose-insensitive β cells from human T2D subjects.

Recent studies report that inhibition of the pentose phosphate pathway enzyme glucose-6-phosphate dehydrogenase (G6PDH) by dehydroepiandrosterone (DHEA) (Spégel et al., 2013), or suppression of the subsequent step in the pathway, 6-phosphogluconate dehydrogenase (6PGDH), by siRNA or the chemical inhibitor 6-AN (Goehring et al., 2011), results in impaired GSIS. The effects of 6PGDH inhibition were ascribed to the accumulation of early pentose shunt pathway intermediates and activation of p-ERK (Goehring et al., 2011), whereas DHEA treatment was reported to cause a decrease in reduced glutathione (GSH) levels, presumably secondary to impaired NADPH production, although the effect of DHEA on NADPH was not reported (Spégel et al., 2013). Here we show that a specific, glucose-regulated product of the pentose shunt and the purine pathway, S-AMP, has a direct effect to augment exocytosis in normal islets, presenting an alternative explanation for these prior findings.

Our data suggest that manipulation of S-AMP levels may provide a means of enhancing secretion in otherwise dysfunctional islets in T2D. Currently, there is very little information available about the impact of T2D on the purine pathway in general, or on S-AMP levels more specifically. Earlier reports showed the inhibitory effect of MPA on GSIS and guanine nucleotide levels, but did not fully recognize the impact of MPA on the adenine branch of nucleotide metabolism and did not identify S-AMP as a regulated metabolite (Li et al., 2000). Another report described altered adenine nucleotide metabolism in the diabetic heart in the BB/Wistar and streptozotocin diabetes rat models, with increases in the AMP catabolic enzymes 5′-nucleotidase, adenosine deaminase, and AMP deaminase, and apparent compensatory induction of the nucleotide cycle enzymes ADSS and ADSL (Jenkins et al., 1988), but islet studies were not reported. More recently, a study of the thiazolidinedione (TZD)/PPARγ activators rosiglitazone and pioglitazone in normal rats revealed increases in cardiac IMP and AMP levels in response to drug treatment, accompanied by transcriptional upregulation of G6PDH, the PRPP-synthesizing enzyme Prps1, and ADSS (Liu et al., 2013), but again S-AMP was not measured and islet studies were not performed. Interestingly, interaction of PPARγ with the ADSS promoter was reported, and TZDs are known to be protective against the development of β cell failure and diabetes in the Zucker diabetic fatty (ZDF) rat (Shimabukuro et al., 1998; Sreenan et al., 1996). Additional studies will be required to define potential changes in the expression of key S-AMP-generating and -degrading enzymes in islets in rodent models and human T2D islets

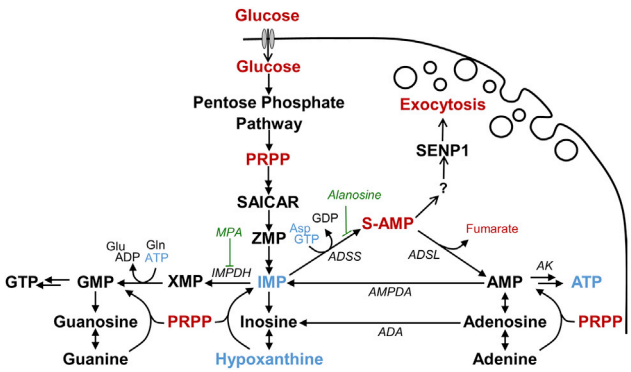


**Figure 7. Schematic Summary of the Role of Purine/Nucleotide Pathways in Coupling of Glucose Metabolism and Insulin Secretion**

The purine metabolic pathway is shown with metabolites that increase (red) or decrease (blue) in response to glucose stimulation in the 832/13 cell line. ADA, adenosine deaminase; ADSL, adenylosuccinate lyase; ADSS, adenylosuccinate synthase; AK, adenylate kinase; AMPDA, AMP deaminase; IMP, inosine monophosphate; IMPDH, inosine 5-monophosphate dehydrogenase; MPA, mycophenolic acid; S-AMP, adenylosuccinate.

and the possible restorative effects of TZD or adenine supplementation in those preparations. Conversely, one potential explanation for the impact of ADSS suppression on GSIS could have been a secondary perturbation of genes known to regulate GSIS or disallowed genes associated with β cell secretory dysfunction (Thorrez et al., 2011). However, we found no changes in the expression of GLUT2; glucokinase; Kir6.2 (component of the $K_{ATP}$ channel); the cytosolic, NADP-dependent isoform of isocitrate dehydrogenase (ICDc); or lactate dehydrogenase (representative of the disallowed genes) in response to ADSS1 or ADSS2 knockdown in four separate biological samples, each assayed in duplicate or triplicate (data not shown).

The classical model of GSIS holds that glucose-induced increases in the ATP:ADP ratio trigger insulin secretion via inhibition of $K_{ATP}$ channels, causing membrane depolarization and activation of voltage-gated $Ca^{2+}$ channels. Evidence for $K_{ATP}$ channel-independent, complementary metabolic signaling pathways in control of GSIS has been mounting steadily (Jensen et al., 2008; MacDonald et al., 2005; Prentki et al., 2013; Gooding et al., 2015). Anaplerotic metabolism of glucose in mitochondria appears to control one such complementary pathway by affecting β cell redox status, GSH:GSSG ratio, and activity of SENP1 (Ferdaoussi et al., 2015; Ivarsson et al., 2005; Jensen et al., 2008; Reinbothe et al., 2009). Here we show that glucose-induced flux through de novo purine synthesis and ADSS2 drive increases in S-AMP levels in β cells, causing enhanced insulin granule exocytosis. During glucose stimulation, the β cell has multiple sources of anaplerotic substrates, including pyruvate entering through pyruvate carboxylase and conversion of glutamine/glutamate to α-ketoglutarate, thus generating sufficient levels of tricarboxylic acid (TCA) cycle intermediates to allow their exit from the mitochondria for engagement in cytosolic, signal-inducing pathways, most notably the pyruvate-isocitrate pathway (Ferdaoussi et al., 2015; Jensen et al., 2008; Ronnebaum et al., 2006). In contrast, in skeletal muscle during exercise, anaplerotic substrates are limited, and activation of the nucleotide cycle through ADSS1 and ADSL is thought to be an important source of the anaplerotic metabolite fumarate, thus sustaining the TCA cycle and ATP production. The data presented herein are consistent with the idea that S-AMP synthesis is an important functional role of the nucleotide cycle in islets, allowing S-AMP to act as a glucose-induced amplifying signal for insulin granule exocytosis (see Figure 7 for schematic summary).

Given the important role assigned to changes in the ATP:ADP ratio in control of GSIS in the historical literature, can we separate the proposed signaling role of S-AMP from changes in these other nucleotides? Several of our observations support a specific role for S-AMP. (1) Alanosine-mediated inhibition of ADSS causes decreases in levels of S-AMP, ADP, and ATP, while also causing impairment of GSIS. The suppression of GSIS can be rescued by the provision of adenine, which causes S-AMP, ADP, and ATP levels to return to normal (Figure 3). The [ATP]/[ADP] ratio in both the suppressed and rescued states is similar, arguing against a key role for this variable in mediating the observed changes in GSIS under these conditions. (2) As shown in Figure 5, silencing of ADSL results in a specific lowering of S-AMP in concert with impairment of GSIS, with no decreases in ADP or ATP levels or changes in ATP:ADP ratio. (3) In studies with patch-clamped rat insulinoma and human β cells shown in Figures 4 and 6, ATP levels are fixed and $K_{ATP}$ channel regulation does not occur because membrane potential is clamped in this experimental system. Despite this, S-AMP exhibits a strong effect to amplify insulin granule exocytosis in the patch-clamped cells. We also note that other metabolic intermediates in addition to ATP, ADP, and changes in the ratios of these nucleotides have been considered as mediators of GSIS. Our study focused on the purine/nucleotide pathway, but the reader is referred to a recent review for discussion of other implicated metabolites and pathways (Gooding et al., 2015).

The fundamental question of how S-AMP interacts with the downstream secretory machinery to affect granule exocytosis remains to be resolved. Insulin granule exocytosis is impaired by attachment of SUMO peptides to secretory granules, and nutrient stimulation activates SENP1 to remove these modifications and activate secretion (Dai et al., 2011; Vergari et al., 2012). We recently have demonstrated that GSH/glutaredoxin interact with cysteine residues required for SENP1 catalytic function, and that the stimulatory effects of isocitrate or GSH on amplification of exocytosis require SENP1 (Ferdaoussi et al., 2015). Here we show that the amplifying effect of S-AMP on exocytosis also is dependent on SENP1 activity. Whether the S-AMP/SENP1 signaling pathway represents an independent or convergent pathway relative to the pyruvate-isocitrate-GSH-SENP1 pathway remains to be investigated.

In sum, our findings have identified a potent glucose-derived secretagogue from the purine biosynthesis pathway. Future work will be focused on probing this pathway as a potential source of targets for improving β cell function in T2D.

## EXPERIMENTAL PROCEDURES

### Reagents, Cell Lines, and Primary Islets

All reagents and solutions were obtained from Sigma-Aldrich unless otherwise indicated. The rat insulinoma cell line 832/13 was cultured as described

previously (Hohmeier et al., 2000). Rat islets were harvested from male Sprague-Dawley rats weighing ~300 g under a protocol approved by the Duke University Institutional Animal Care and Use Committee and cultured as described previously (Ronnebaum et al., 2008). Human islets were isolated from pancreata of non-diabetic organ donors (n = 6) and a donor with T2D (n = 1) at the Alberta Diabetes Institute Islet Core, as previously described (Kin and Shapiro, 2010). All studies with human islets were approved by the Human Research Ethics Board (Pro00001754) at the University of Alberta. All organ donors provided informed consent for use of pancreatic tissue in research (Pro00013094).

### GSIS

Insulin secretion from 832/13 cells and rat islets (~20 islets per incubation) was measured as described previously (Jensen et al., 2006) by radioimmunoassay (RIA) (Siemens) or ELISA (ALPCO). For GSIS from human islets, human islet cell aggregate cultures were prepared and used as described in the Supplemental Experimental Procedures.

### IMPDH and ADSS Inhibition Experiments

For IMPDH inhibition experiments in confluent 832/13 cells, 0.1% ethanol or MPA was added to the culture media overnight and was included during pre-incubation and GSIS as well, with or without adenine (250 μM), guanine (100 μM), or 0.125 N NaOH. For ADSS inhibition, L/D-alanosine (Santa Cruz Biotechnology) was dissolved in 50 mM HEPES (pH 8.6) at several concentrations and added to confluent 832/13 cells or whole rat islets, in the presence and absence of 100 μM adenine, overnight and during performance of the GSIS assays. Controls were treated with equal volumes of 50 mM HEPES (pH 8.6).

### siRNA-Mediated Gene Silencing of ADSS1, ADSS2, and ADSL and Quantitative Real-Time PCR Analyses

Methods and siRNA duplex sequences used for silencing of ADSS1, ADSS2, and ADSL in 832/13 cells, as well as the methods used for quantitative real-time PCR analyses, are provided in the Supplemental Experimental Procedures.

### Cell Harvest for Nucleotide Extraction

After 2 hr of GSIS, media were removed and 832/13 cells were scraped from plates in secretion buffer into a 15-ml conical tube and centrifuged. The cell pellet was flash frozen in a dry-ice ethanol bath. A cold solution of methanol (200 μl) containing nine internal standards ($^{13}C_{10}$, $^{15}N_5$-AMP [90 μM]; $^{13}C_{10}$, $^{15}N_5$-GMP [30 μM]; $^{13}C_{10}$, $^{15}N_2$-UMP [15 μM]; $^{13}C_9$, $^{15}N_3$-CMP [15 μM]; $^{13}C_{10}$-GTP [30 μM]; $^{13}C_{10}$-UTP [45 μM]; $^{13}C_9$-CTP [15 μM]; $^{13}C_{10}$-ATP [300 μM]; and nicotinamide-1,N6-ethenoadenine dinucleotide [εNAD, 75 μM]) was added and the pellets were allowed to thaw on ice before resuspension by pipetting. Chilled water (100 μl) and then hexane (300 μl) were added to each tube, and the tubes were vortexed vigorously and centrifuged. The bottom aqueous layer was collected and centrifuged again. The supernatants were transferred to a 96-well plate for analysis by LC-MS/MS.

### LC-MS/MS

The method is a modification of a previously published approach (Cordell et al., 2008). Chromatographic separations were performed using an Agilent Technologies 1200 HPLC system and a Chromolith FastGradient RP-18e 50-2mm column (EMD Millipore). Injection volume was 2 μl. Mobile phase A was 95% water, 5% methanol, and 5 mM dimethylhexylamine adjusted to pH 7.5 with acetic acid. Mobile phase B was 20% water, 80% methanol, and 10 mM dimethylhexylamine. Flow rate was set to 0.3 ml/min and column temperature was 40°C. A 22-min gradient method (t = 0, %B = 0; t = 1.2, %B = 0; and t = 22, %B = 40) was run followed by a 3-min wash and 7-min equilibration. Flow was directed to an Agilent 6410 Triple Quadrupole mass spectrometer and source conditions were set to 4,000 V capillary voltage, 350°C gas temperature, 12 l/min gas flow, and 30 psi nebulizer flow. All nucleotides were detected in negative ion MRM mode based on a characteristic fragmentation reaction (see Table S1). Quantitation of metabolites used nine isotope-labeled internal standards and an external calibration using serial dilution of nucleotide standards.

### Single-Cell Measurement of β Cell Exocytosis

For patch-clamping experiments, islets were cultured in low-glucose (5.5 mM) DMEM with L-glutamine, 110 mg/l sodium pyruvate, 10% fetal bovine serum (FBS), and 100 U/ml penicillin/streptomycin. For SENP1 siRNA studies in human β cells, siRNA duplexes were transfected into dissociated human islet cells with Dharmafect Transfection Reagent 1. The siSenp1 was obtained from Life Technologies (s26615) and a scrambled siRNA (siScrambled; Allstars negative control siRNA, QIAGEN) was used as the control. Dissociated human islet cells or 832/13 cells were plated on 35-mm dishes overnight or for 72 hr in the case of SENP1 knockdown experiments. Prior to patch-clamping, cells were pre-incubated in DMEM (human) or RPMI-1640 (832/13) media with 1 mM glucose for 1 hr and then exposed to patch-clamp bath solution with either 1 or 10 mM glucose for ~15 min. Whole-cell patch-clamp was performed after this, according to previously published methods (Dai et al., 2011; Ferdaoussi et al., 2015) and as outlined in the Supplemental Experimental Procedures.

### Statistical Analyses

For insulin secretion, relative expression, and exocytosis experiments, statistical significance was determined by two-sample, unpaired equal variance Student's t test. The statistical significance of metabolite concentrations was analyzed using the Wilcoxon rank-sum test to allow for a non-normal distribution of values due to experimental batch effects (Bauer, 1972). The Wilcoxon test was completed using the wilcox.test function in R (R-Core Team, 2014). In all cases p values of $<0.05$ were considered significant.

## SUPPLEMENTAL INFORMATION

Supplemental Information includes Supplemental Experimental Procedures, two figures, and one table and can be found with this article online at http://dx.doi.org/10.1016/j.celrep.2015.08.072.

## AUTHOR CONTRIBUTIONS

J.R.G., M.V.J., P.E.M., and C.B.N. designed the study. J.R.G. and B.R.W. performed metabolomics analyses. M.V.J. performed gene knockdown and insulin secretion studies in 832/13 cells, rat islets, and human islet cell cultures. D.L. isolated and purified rat islets, and R.A. helped develop human islet cell culture techniques and assisted M.V.J. in studies with such preparations. X.D. and M.F. performed patch-clamp studies and SENP1 knockdown studies in 832/13 cells and human islets, including T2D islets. J.R.G., M.V.J., P.E.M., and C.B.N. analyzed data. J.R.G., M.V.J., and C.B.N. wrote the paper, and J.R.G., M.V.J., P.E.M., and C.B.N. edited and finalized the paper.

## ACKNOWLEDGMENTS

The authors thank the Human Organ Procurement and Exchange (HOPE) program and Trillium Gift of Life Network (TGLN) for their efforts in procuring human organs for research; Mr. James Lyon (University of Alberta) for his efforts in human islet isolation; Ms. Helena Winfield for assistance with rat islet isolation; and Drs. Lisa Norquay, Jeff Trimmer, and Julia Brosnan (Pfizer Cardiovascular and Metabolic Disease Unit) for sharing methods for studying human islet cell aggregate cultures. This work was funded by NIH grant DK046492-22 (to C.B.N.), NIH grant K01GM109320-02 (to J.R.G.), and Canadian Institutes of Health Research (CIHR) grant MOP 244739 (to P.E.M.). P.E.M. holds a Canada Research Chair in Islet Biology.

Received: May 11, 2015
Revised: August 4, 2015
Accepted: August 26, 2015
Published: September 24, 2015

## REFERENCES

Bauer, D.F. (1972). Constructing confidence sets using rank statistics. J. Am. Stat. Assoc. *67*, 687–690.

Bryan, J., Crane, A., Vila-Carriles, W.H., Babenko, A.P., and Aguilar-Bryan, L. (2005). Insulin secretagogues, sulfonylurea receptors and K(ATP) channels. Curr. Pharm. Des. *11*, 2699–2716.

Carr, S.F., Papp, E., Wu, J.C., and Natsumeda, Y. (1993). Characterization of human type I and type II IMP dehydrogenases. J. Biol. Chem. *268*, 27286–27290.

Cordell, R.L., Hill, S.J., Ortori, C.A., and Barrett, D.A. (2008). Quantitative profiling of nucleotides and related phosphate-containing metabolites in cultured mammalian cells by liquid chromatography tandem electrospray mass spectrometry. J. Chromatogr. B Analyt. Technol. Biomed. Life Sci. *871*, 115–124.

Dai, X.Q., Plummer, G., Casimir, M., Kang, Y., Hajmrle, C., Gaisano, H.Y., Manning Fox, J.E., and MacDonald, P.E. (2011). SUMOylation regulates insulin exocytosis downstream of secretory granule docking in rodents and humans. Diabetes *60*, 838–847.

Detimary, P., Van den Berghe, G., and Henquin, J.C. (1996). Concentration dependence and time course of the effects of glucose on adenine and guanine nucleotides in mouse pancreatic islets. J. Biol. Chem. *271*, 20559–20565.

El-Azzouny, M., Evans, C.R., Treutelaar, M.K., Kennedy, R.T., and Burant, C.F. (2014). Increased glucose metabolism and glycerolipid formation by fatty acids and GPR40 receptor signaling underlies the fatty acid potentiation of insulin secretion. J. Biol. Chem. *289*, 13575–13588.

Ferdaoussi, M., Dai, X., Jensen, M.V., Wang, R., Peterson, B.S., Huang, C., Ilkayeva, O., Smith, N., Miller, N., Hajmrle, C., et al. (2015). Isocitrate-to-SENP1 signaling amplifies insulin secretion and rescues dysfunctional b-cells. J. Clin. Invest. *125*, Published online September 21, 2015. http://dx.doi.org/10.1172/JCI82498.

Gembal, M., Gilon, P., and Henquin, J.C. (1992). Evidence that glucose can control insulin release independently from its action on ATP-sensitive K+ channels in mouse B cells. J. Clin. Invest. *89*, 1288–1295.

Goehring, I., Sauter, N.S., Catchpole, G., Assmann, A., Shu, L., Zien, K.S., Moehlig, M., Pfeiffer, A.F., Oberholzer, J., Willmitzer, L., et al. (2011). Identification of an intracellular metabolic signature impairing beta cell function in the rat beta cell line INS-1E and human islets. Diabetologia *54*, 2584–2594.

Gooding, J.R., Jensen, M.V., and Newgard, C.B. (2015). Metabolomics applied to the pancreatic islet. Arch. Biochem. Biophys. S0003-9861(15)00277-5. http://dx.doi.org/10.1016/j.abb.2015.06.013.

Hager, P.W., Collart, F.R., Huberman, E., and Mitchell, B.S. (1995). Recombinant human inosine monophosphate dehydrogenase type I and type II proteins. Purification and characterization of inhibitor binding. Biochem. Pharmacol. *49*, 1323–1329.

Henquin, J.C., Ravier, M.A., Nenquin, M., Jonas, J.C., and Gilon, P. (2003). Hierarchy of the beta-cell signals controlling insulin secretion. Eur. J. Clin. Invest. *33*, 742–750.

Hohmeier, H.E., Mulder, H., Chen, G., Henkel-Rieger, R., Prentki, M., and Newgard, C.B. (2000). Isolation of INS-1-derived cell lines with robust ATP-sensitive K+ channel-dependent and -independent glucose-stimulated insulin secretion. Diabetes *49*, 424–430.

Huang, M., and Joseph, J.W. (2014). Assessment of the metabolic pathways associated with glucose-stimulated biphasic insulin secretion. Endocrinology *155*, 1653–1666.

Ivarsson, R., Quintens, R., Dejonghe, S., Tsukamoto, K., in 't Veld, P., Renström, E., and Schuit, F.C. (2005). Redox control of exocytosis: regulatory role of NADPH, thioredoxin, and glutaredoxin. Diabetes *54*, 2132–2142.

Jayaram, H.N., Tyagi, A.K., Anandaraj, S., Montgomery, J.A., Kelley, J.A., Kelley, J., Adamson, R.H., and Cooney, D.A. (1979). Metabolites of alanosine, an antitumor antibiotic. Biochem. Pharmacol. *28*, 3551–3566.

Jenkins, R.L., McDaniel, H.G., Digerness, S., Parrish, S.W., and Ong, R.L. (1988). Adenine nucleotide metabolism in hearts of diabetic rats. Comparison to diaphragm, liver, and kidney. Diabetes *37*, 629–636.

Jensen, M.V., Joseph, J.W., Ilkayeva, O., Burgess, S., Lu, D., Ronnebaum, S.M., Odegaard, M., Becker, T.C., Sherry, A.D., and Newgard, C.B. (2006). Compensatory responses to pyruvate carboxylase suppression in islet beta-cells. Preservation of glucose-stimulated insulin secretion. J. Biol. Chem. *281*, 22342–22351.

Jensen, M.V., Joseph, J.W., Ronnebaum, S.M., Burgess, S.C., Sherry, A.D., and Newgard, C.B. (2008). Metabolic cycling in control of glucose-stimulated insulin secretion. Am. J. Physiol. Endocrinol. Metab. *295*, E1287–E1297.

Joseph, J.W., Jensen, M.V., Ilkayeva, O., Palmieri, F., Alárcon, C., Rhodes, C.J., and Newgard, C.B. (2006). The mitochondrial citrate/isocitrate carrier plays a regulatory role in glucose-stimulated insulin secretion. J. Biol. Chem. *281*, 35624–35632.

Kanno, T., Ma, X., Barg, S., Eliasson, L., Galvanovskis, J., Göpel, S., Larsson, M., Renström, E., and Rorsman, P. (2004). Large dense-core vesicle exocytosis in pancreatic beta-cells monitored by capacitance measurements. Methods *33*, 302–311.

Kin, T., and Shapiro, A.M. (2010). Surgical aspects of human islet isolation. Islets *2*, 265–273.

Kitchin, J.E., Pomeranz, M.K., Pak, G., Washenik, K., and Shupack, J.L. (1997). Rediscovering mycophenolic acid: a review of its mechanism, side effects, and potential uses. J. Am. Acad. Dermatol. *37*, 445–449.

Li, G.D., Luo, R.H., and Metz, S.A. (2000). Effects of inhibitors of guanine nucleotide synthesis on membrane potential and cytosolic free Ca2+ levels in insulin-secreting cells. Biochem. Pharmacol. *59*, 545–556.

Liu, Y., Yan, X., Mao, G., Fang, L., Zhao, B., Liu, Y., Tang, H., and Wang, N. (2013). Metabonomic profiling revealed an alteration in purine nucleotide metabolism associated with cardiac hypertrophy in rats treated with thiazolidinediones. J. Proteome Res. *12*, 5634–5641.

Lorenz, M.A., El Azzouny, M.A., Kennedy, R.T., and Burant, C.F. (2013). Metabolome response to glucose in the β-cell line INS-1 832/13. J. Biol. Chem. *288*, 10923–10935.

Lu, D., Mulder, H., Zhao, P., Burgess, S.C., Jensen, M.V., Kamzolova, S., Newgard, C.B., and Sherry, A.D. (2002). 13C NMR isotopomer analysis reveals a connection between pyruvate cycling and glucose-stimulated insulin secretion (GSIS). Proc. Natl. Acad. Sci. USA *99*, 2708–2713.

MacDonald, M.J., Fahien, L.A., Brown, L.J., Hasan, N.M., Buss, J.D., and Kendrick, M.A. (2005). Perspective: emerging evidence for signaling roles of mitochondrial anaplerotic products in insulin secretion. Am. J. Physiol. Endocrinol. Metab. *288*, E1–E15.

Muoio, D.M., and Newgard, C.B. (2008). Mechanisms of disease:Molecular and metabolic mechanisms of insulin resistance and beta-cell failure in type 2 diabetes. Nat. Rev. Mol. Cell Biol. *9*, 193–205.

Natsumeda, Y., Ohno, S., Kawasaki, H., Konno, Y., Weber, G., and Suzuki, K. (1990). Two distinct cDNAs for human IMP dehydrogenase. J. Biol. Chem. *265*, 5292–5295.

Newgard, C.B., and Matschinsky, F.M. (2001). Substrate control of insulin release. In Handbook of Physiology, *Volume A*, J. Jefferson, ed. (Oxford University Press), pp. 125–152.

Prentki, M., Matschinsky, F.M., and Madiraju, S.R. (2013). Metabolic signaling in fuel-induced insulin secretion. Cell Metab. *18*, 162–185.

R-Core Team (2014). R: a language and environment for statistical computing. http://www.R-project.org/.

Reinbothe, T.M., Ivarsson, R., Li, D.Q., Niazi, O., Jing, X., Zhang, E., Stenson, L., Bryborn, U., and Renström, E. (2009). Glutaredoxin-1 mediates NADPH-dependent stimulation of calcium-dependent insulin secretion. Mol. Endocrinol. *23*, 893–900.

Ronnebaum, S.M., Ilkayeva, O., Burgess, S.C., Joseph, J.W., Lu, D., Stevens, R.D., Becker, T.C., Sherry, A.D., Newgard, C.B., and Jensen, M.V. (2006). A pyruvate cycling pathway involving cytosolic NADP-dependent isocitrate dehydrogenase regulates glucose-stimulated insulin secretion. J. Biol. Chem. *281*, 30593–30602.

Ronnebaum, S.M., Jensen, M.V., Hohmeier, H.E., Burgess, S.C., Zhou, Y.P., Qian, S., MacNeil, D., Howard, A., Thornberry, N., Ilkayeva, O., et al. (2008). Silencing of cytosolic or mitochondrial isoforms of malic enzyme has no effect

on glucose-stimulated insulin secretion from rodent islets. J. Biol. Chem. *283*, 28909–28917.

Sato, Y., Aizawa, T., Komatsu, M., Okada, N., and Yamada, T. (1992). Dual functional role of membrane depolarization/Ca2+ influx in rat pancreatic B-cell. Diabetes *41*, 438–443.

Shimabukuro, M., Zhou, Y.T., Lee, Y., and Unger, R.H. (1998). Troglitazone lowers islet fat and restores beta cell function of Zucker diabetic fatty rats. J. Biol. Chem. *273*, 3547–3550.

Spégel, P., Malmgren, S., Sharoyko, V.V., Newsholme, P., Koeck, T., and Mulder, H. (2011). Metabolomic analyses reveal profound differences in glycolytic and tricarboxylic acid cycle metabolism in glucose-responsive and -unresponsive clonal β-cell lines. Biochem. J. *435*, 277–284.

Spégel, P., Sharoyko, V.V., Goehring, I., Danielsson, A.P., Malmgren, S., Nagorny, C.L., Andersson, L.E., Koeck, T., Sharp, G.W., Straub, S.G., et al. (2013). Time-resolved metabolomics analysis of β-cells implicates the pentose phosphate pathway in the control of insulin release. Biochem. J. *450*, 595–605.

Sreenan, S., Sturis, J., Pugh, W., Burant, C.F., and Polonsky, K.S. (1996). Prevention of hyperglycemia in the Zucker diabetic fatty rat by treatment with metformin or troglitazone. Am. J. Physiol. *271*, E742–E747.

Stayton, M.M., Rudolph, F.B., and Fromm, H.J. (1983). Regulation, genetics, and properties of adenylosuccinate synthetase: a review. Curr. Top. Cell. Regul. *22*, 103–141.

Straub, S.G., and Sharp, G.W. (2002). Glucose-stimulated signaling pathways in biphasic insulin secretion. Diabetes Metab. Res. Rev. *18*, 451–463.

Thorrez, L., Laudadio, I., Van Deun, K., Quintens, R., Hendrickx, N., Granvik, M., Lemaire, K., Schraenen, A., Van Lommel, L., Lehnert, S., et al. (2011). Tissue-specific disallowance of housekeeping genes: the other face of cell differentiation. Genome Res. *21*, 95–105.

Vergari, E., Plummer, G., Dai, X., and MacDonald, P.E. (2012). DeSUMOylation Controls Insulin Exocytosis in Response to Metabolic Signals. Biomolecules *2*, 269–281.

Yeh, E.T. (2009). SUMOylation and De-SUMOylation: wrestling with life's processes. J. Biol. Chem. *284*, 8223–8227.